J Cardiovasc Imaging. 2019 Jan;27(1):50-63
https://doi.org/10.4250/jcvi.2019.27.e4
pISSN 2586-7210·eISSN 2586-7296

Journal of Cardiovascular Imaging JCVI

Original Article

Differential Transcriptome Profile and Exercise Capacity in Cardiac Remodeling by Pressure Overload versus Volume Overload

Kyung-Hee Kim, MD, PhD[1], Hyue-Mee Kim, MD[1], Jin-Sik Park, MD[1], and Yong-Jin Kim, MD, PhD[2]

[1]Department of Internal Medicine, Cardiovascular Center, Sejong General Hospital, Incheon, Korea
[2]Department of Internal Medicine, Seoul National University College of Medicine, Seoul National University Hospital, Seoul, Korea

Received: Nov 19, 2018
Revised: Dec 7, 2018
Accepted: Dec 21, 2018

Address for Correspondence:
Yong-Jin Kim, MD, PhD
Department of Internal Medicine, Seoul National University College of Medicine, Cardiovascular Center, Seoul National University Hospital, 101 Daehak-ro, Jongno-gu, Seoul 03080, Korea.
E-mail: kimdamas@snu.ac.kr

ORCID iDs
Kyung-Hee Kim
https://orcid.org/0000-0003-0708-8685
Hyue-Mee Kim
https://orcid.org/0000-0001-7680-6690
Jin-Sik Park
https://orcid.org/0000-0002-6583-9769
Yong-Jin Kim
https://orcid.org/0000-0002-0760-0522

Conflict of Interest
The authors have no financial conflicts of interest.

ABSTRACT

BACKGROUND: We compared the gene expression profiles in the hypertrophied myocardium of rats subjected to pressure overload (PO) and volume overload (VO) using DNA chip technology, and compared the effects on exercise capacity with a treadmill test.
METHODS: Constriction of the abdominal aorta or mitral regurgitation induced by a hole in the mitral leaflet were used to induce PO (n = 19), VO (n = 16) or PO + VO (n = 20) in rats. Serial echocardiographic studies and exercise were performed at 2-week intervals, and invasive hemodynamic examination by a pressure-volume catheter system was performed 12 weeks after the procedure. The gene expression profiles of the left ventricle (LV) 12 weeks after the procedure were analyzed by DNA chip technology.
RESULTS: In hemodynamic analyses, the LV end-diastolic pressure and the end-diastolic pressure-volume relationship slope were greater in the PO group than in the VO group. When we compared LV remodeling and exercise capacity, cardiac fibrosis and exercise intolerance developed in the PO group but not in the VO group (exercise duration, 434.0 ± 80.3 vs. 497.8 ± 49.0 seconds, $p < 0.05$, respectively). Transcriptional profiling of cardiac apical tissues revealed that gene expression related to the inflammatory response and cellular signaling pathways were significantly enriched in the VO group, whereas cardiac fibrosis, cytoskeletal pathway and G-protein signaling genes were enriched in the PO group.
CONCLUSIONS: We found that many genes were regulated in PO, VO or both, and that there were different regulation patterns by cardiac remodeling. Cardiac fibrosis and cytoskeletal pathway were important pathways in the PO group and influenced exercise capacity. Cardiac fibrosis influences exercise capacity before LV function is reduced.

Keywords: Pressure overload; Volume overload; Cardiac fibrosis; Exercise capacity

INTRODUCTION

Myocardial hypertrophy is a morphological adaptive response to chronic work overload imposed on the heart. It has been categorized into two distinct basic types: concentric hypertrophy, occurring in response to a sustained pressure overload (PO) in which wall thickness increases without chamber enlargement, and eccentric hypertrophy, in response

Journal of Cardiovascular Imaging JCVI

to a chronic volume overload (VO) in which chamber volume enlarges without a relative increase in its wall thickness.[1] At the cellular level, cardiomyocytes grow vertically in PO and longitudinally in VO. The molecular mechanisms for this difference have not been determined. It is thought that some specific genes are regulated similarly or differentially in PO and VO, but the regulation of genes other than those listed above has not been clarified. Microarray analysis is a useful method to analyze the behavior of many genes at once. With this method, gene expression profiling has been conducted in animal hearts subjected to PO.[2][3] However, this has not been conducted in hearts subjected to VO. The character, degree, and duration of the work induced by an overload, itself produced by volume and/or pressure, play a critical role in determining the course of the process of hypertrophy. The cardiac hypertrophy induced by overload through a change in volume as opposed to pressure may be distinctly different biological phenomena, mediated through different mechanisms. We compared the gene expression profiles in the hypertrophied myocardium of rats subjected to PO, VO or both using DNA chip technology, and compared the effects on exercise capacity with treadmill testing. Additionally, in the present study, we assessed the contribution of PO and its associated diastolic dysfunction to left ventricular (LV) remodeling and exercise capacity in a rat animal model with significant VO.

METHODS

Animal model

All of the rats were housed in the Laboratory Animal Facility of the Clinical Research Institute of Seoul National University Hospital. The study protocol was approved by the Institutional Animal Care and Use Committee of Seoul National University Hospital.

An animal model of PO

To develop the animal model of PO and diastolic dysfunction, we used suprarenal aortic constriction (PO, 19). At the age of 11 weeks, 8Sprague-Dawley rats (350-400 g) were placed in a 1-L gas anesthetic chamber and subjected to an induction of 5% isoflurane at a rate of 4 L/min oxygen. Then, they were intubated and ventilated using a respirator. Anesthesia was maintained by mixing isoflurane with oxygen (2% isoflurane at a rate of 2 L/min oxygen). Suprarenal aortic constriction was performed with a 4-0 silk tie around a blunt 22-gauge probe (0.6-mm outer diameter) just above the right renal artery. The probe was promptly removed after constriction.[4] At 2-week intervals after the surgery, echocardiography was performed to confirm the development of LV hypertrophy (LVH) and diastolic dysfunction. At 12 weeks after suprarenal aortic constriction, invasive hemodynamic monitoring was performed using a Millar catheter system for confirming the development of diastolic dysfunction.

An animal model of VO with/without PO

To develop the animal model of VO, we used a mitral regurgitation (MR) model. The rats were divided into 3 groups. For the VO + PO group (n = 20), PO was performed at the age of 11 weeks as described above, and MR was induced at 2 weeks after PO. In the VO (MR) group (n = 16), at the same time point of PO, laparotomy was performed instead of suprarenal aortic ligation, and then VO (MR) was induced at the age of 13 weeks. In the sham group (n = 14), only a sham operation was performed:laparotomy and thoracotomy followed by apical puncture.

MR was surgically induced under the guidance of transesophageal echocardiography, as we have already published.[5][6]

https://doi.org/10.4250/jcvi.2019.27.e4

Journal of Cardiovascular Imaging JCVI

Transthoracic echocardiography

Echocardiography was performed at baseline (11 weeks of age), 2 weeks after PO (13 weeks of age), 3 weeks after creation of MR (16 weeks of age), 19, 21, and 25 weeks of age. The rats were anesthetized in the previously described manner and placed on a ventilator for mechanical ventilation. Images were acquired with a 12-MHz transducer connected to a Vivid i echocardiography machine (GE Medical, Milwaukee, WI, USA). M-mode and 2-dimensional echocardiography images at the papillary muscle level were acquired with a frame rate of 200 or more per second. LV end-diastolic septal and posterior wall thickness (IVS and PW), LV end-diastolic dimension (LVEDD) and LV end-systolic dimension (LVESD) were measured. The LV ejection fraction (LVEF) was calculated according to the following formula: LVEF = (LVEDD^2 - LVESD^2) / LVEDD^2. All parameters were evaluated on an average of three consecutive beats. A single echocardiographer who was blinded to the treatment information of the animals performed all of the data acquisition.

Hemodynamic measurements

Anesthesia was initiated with isoflurane inhalation. The animals were intubated with a blunt 16-gauge needle via tracheostomy, and were ventilated with a custom designed constant-pressure ventilator at 75 breaths/min using room air. The chest was entered through an anterior thoracotomy, and a small apical stab was made to expose the LV apex. After an apical puncture with a 27-gauge needle, the pressure-volume (P-V) catheter (SPR-838, Millar Instruments; Houston, TX, USA) was advanced retrogradely into the LV cavity along the cardiac longitudinal axis until stable P-V loops were obtained.[7]

Exercise test

Maximal exercise capacity was evaluated with a Rota Rod treadmill (Ugo Basile, Comerio, Italy), in which rats run on a knurled drum as the drum rotates to avoid falling off. Animals were trained twice before the test to become familiar with the treadmill. Treadmill speed was gradually increased from 3 to 15 rpm every 1 minute. Exercise time was recorded. The observer blinded to the study group recorded episodes of the immobility response that resulted from exhaustion. The detailed experimental protocol is shown in **Figure 1**.

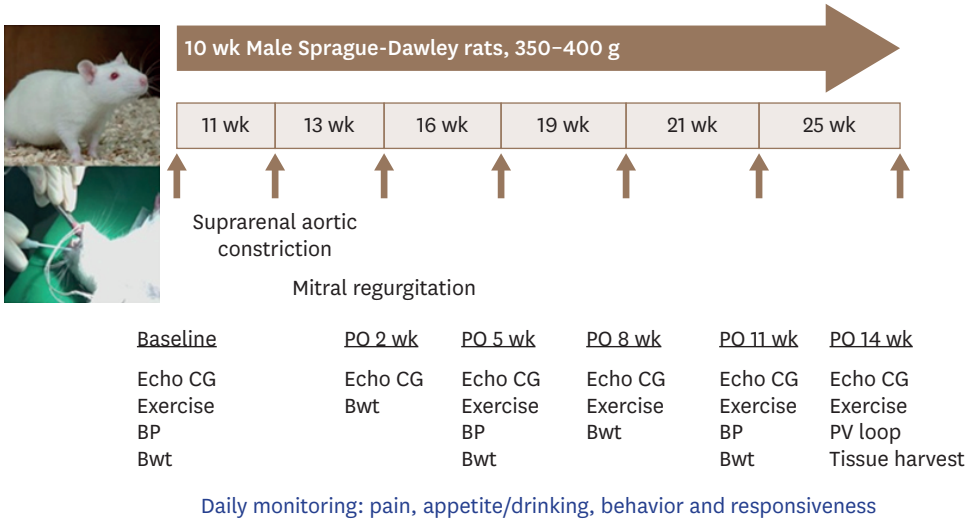

Figure 1. Schematic illustration of experimental protocol. BP: blood pressure, Bwt: body weight, ECG: echocardiography, PO: pressure overload, PV: pressure-volume, wk: week.

https://doi.org/10.4250/jcvi.2019.27.e4

Journal of Cardiovascular Imaging JCVI

Histological analysis

After hemodynamic measurements were performed, the rats were euthanized, the hearts and lungs were harvested and weighed and the apical scar was excluded.

RNA isolation

Fresh LV apex, excluding the apical scar, was immediately stored in RNAlater (Ambion/Applied Biosciences, Streetsville, ON, Canada) at −80°C until use. The hearts were homogenized in TRIzol reagent (Invitrogen, Burlington, ON, Canada), and total RNA was isolated according to the manufacturer's instructions. RNA was further purified to remove genomic DNA contamination and was concentrated with the use of an RNeasy Plus Mini Kit (Qiagen, Mississauga, ON, Canada). Samples with optical density ratio 260/280 > 1.8, 28S/18S > 1.6 measured with the use of a Bioanalyzer 2100 (Agilent, Santa Clara, CA, USA) were selected for microarray processing.

Microarray analysis

Apical heart RNA excluding scar tissue was labeled with either cyanine 3-CTP (Cy3) or cyanine 5-CTP (Cy5) (PerkinElmer, Boston, MA, USA) with the Low RNA Input Fluorescent Linear Amplification Kit (Agilent Technologies and hybridized onto an Agilent whole rat genome array (G4131A). RNA samples from 3 rats in each group were pooled and hybridized onto 1 chip. The arrays were scanned at 2 different intensities, and the images were analyzed for background correction. BMP4 and FGF2 samples were cohybridized with RNA from the starting point, and a dye swap was performed. The arrays were normalized, and the differential gene expression was analyzed by the R and bioconductor-based method LIMMA. We performed gene set enrichment analysis to find molecular pathways or gene ontologies that are made up of differentially expressed genes in each biological condition. Gene sets with high absolute enrichment score values are molecular pathways or gene ontologies that are made up of upregulated or downregulated genes and are differentially regulated pathways. P values for the enrichment scores were calculated after permuting class labels of each experimental condition, and gene sets with p values < 0.05 were extracted.

Immunohistochemical analysis

Mid ventricles were removed for histopathology and were preserved in 4% paraformaldehyde and embedded in paraffin. The tissue was sectioned into 4-μm sections and stained with Masson's Trichrome for evaluation of the degree of fibrosis for measurement of collagen deposition. The area of interstitial fibrosis was identified after excluding the vessel area from the region of the interest, as the ratio of interstitial fibrosis to the total tissue area.

Statistical analysis

The results are expressed as means ± standard deviation. The Mann-Whitney test or unpaired 2-tailed t test was used to compare continuous variables. For the differences between 3 groups, one-way ANOVA with Tukey's post hoc multiple analysis was used. Repeated-measures ANOVA was performed to analyze the changes of several variables over time LVEF, LV dimension, LV mass index, and exercise capacity. Survival data were evaluated by the Kaplan–Meier method with pairwise comparison conducted with the log-rank test. All calculations were performed using SPSS version 17.0, and p values of < 0.05 were considered statistically significant.

https://doi.org/10.4250/jcvi.2019.27.e4

Journal of Cardiovascular Imaging JCVI

RESULTS

Animal model of diastolic dysfunction (PO model)

First, we confirmed the formation of LVH and diastolic dysfunction in the PO rat model. When we followed up until 14 weeks after suprarenal ligation, LVH had developed (**Figure 2**). LVESD, LVEDD, and LVEF did not become different between the sham group and the PO group. However, IVS thickness increased from 5 weeks after suprarenal artery constriction, and was thicker in the PO group than in the sham group until 8 weeks of suprarenal artery constriction (IVS thickness at 5 weeks after suprarenal constriction, 1.15 ± 0.05 vs. 1.53 ± 0.14 for sham [n = 14] vs. PO group [n = 19], $p < 0.05$). The PW thickness also increased from 5 weeks after suprarenal artery constriction, and continued until 8 weeks of PO (PW thickness 8 weeks after suprarenal artery constriction, 1.17 ± 0.05 vs. 1.45 ± 0.05 for sham [n = 14] vs. PO group [n = 19], $p < 0.05$). LVEF did not change during the follow-up period.

The effect of diastolic dysfunction on LV remodeling in a rat with significant VO

After confirmation of LVH and diastolic dysfunction through suprarenal artery ligation, we investigated how LV remodeling and exercise capacity changed after the development of significant VO. The rats were divided into 3 groups (PO + VO group = suprarenal artery constriction followed by MR induction [n = 20]; VO group = laparotomy followed by MR induction [n = 16]; sham group = laparotomy followed by thoracotomy and apical puncture [n = 14]). Serial echocardiographic examinations were performed for assessment of LV remodeling (**Figure 3**). The IVS and PW thickness became greater in the PO + VO group than in the sham or VO groups from 2 weeks after suprarenal artery constriction. This was maintained during the study period. From 4 weeks after MR induction, the PO + VO group

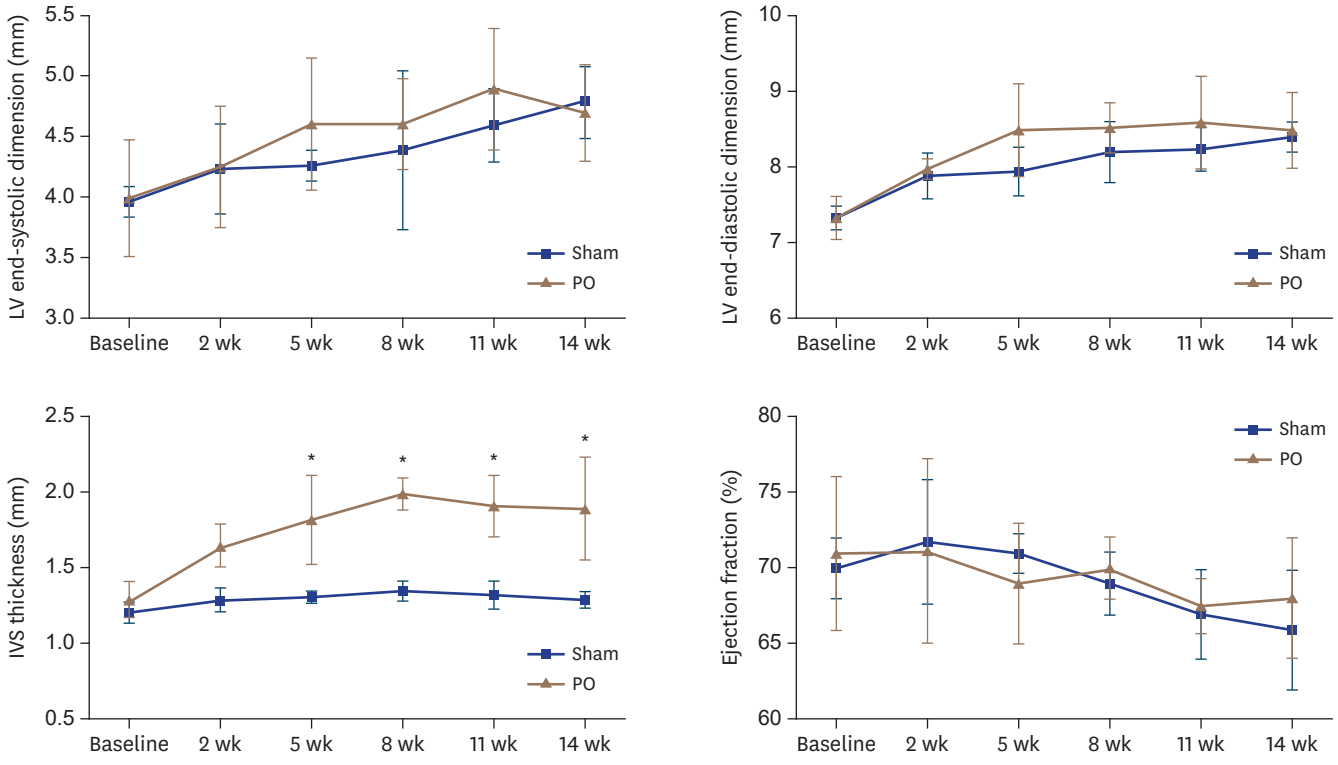

Figure 2. Echocardiographic parameters of PO. IVS: interventricular septum, PO: pressure overload, wk: week.
*$p < 0.05$.

https://doi.org/10.4250/jcvi.2019.27.e4

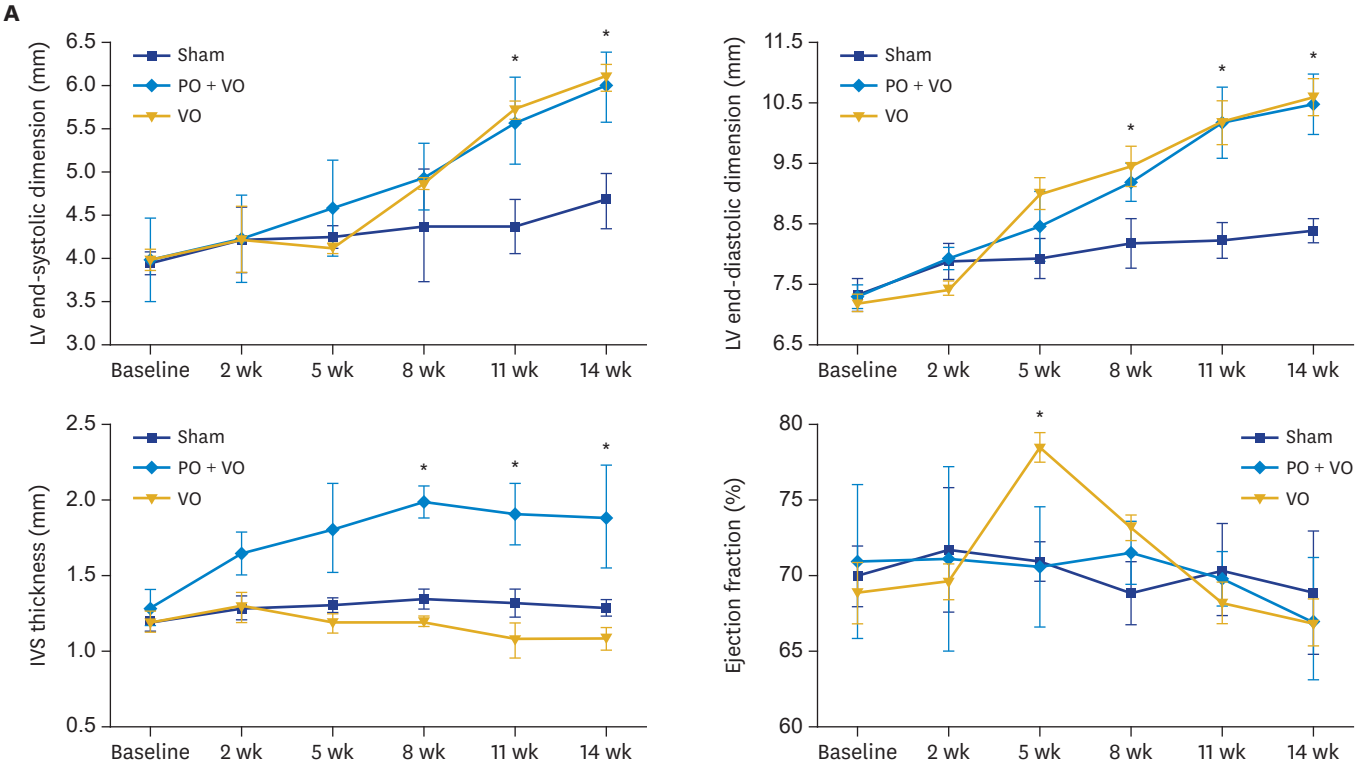

Figure 3. (A) Echocardiographic parameters of PO combined with VO, and VO. (B) A representative image at 14 weeks after PO. IVS: interventricular septum, LV: left ventricular, PO: pressure overload, VO: volume overload, wk: week.

and the VO group had a similar chamber size, even though both groups had a greater chamber size compared with the sham group (LVESD at 9 weeks after MR formation [11 weeks after suprarenal aortic constriction], 4.33 ± 0.26 vs. 5.80 ± 0.40 vs. 5.92 ± 1.38 mm for sham vs. VO vs. PO + VO, $p < 0.05$; LVEDD at the same time, 7.68 ± 0.15 vs. 9.98 ± 0.46 vs. 10.10 ± 1.26 mm, $p < 0.05$; no statistical difference between the PO + VO group and the VO group analyzed by one-way ANOVA with Tukey's post hoc analysis). The LVEF tended to increase immediately

https://doi.org/10.4250/jcvi.2019.27.e4

after MR, suggesting hyperdynamic systolic function, but started to decrease thereafter. At 14 weeks of PO, LVEF slightly but not significantly decreased in the VO group.

Survival analysis

Two rats died of bleeding and one rat died of an unknown cause after surgery, making the postoperative mortality 8%. Three rats died during the acute stage within 2 weeks after the MR surgery due to pulmonary edema and an unknown cause. No death was noted in the sham group. After landmark analysis, a Kaplan–Meier survival curve showed no significance among the sham, PO, VO, and PO + VO groups (**Figure 4A**).

Exercise capacity

Next, we assessed the exercise capacity of the rats by measuring the treadmill time to exhaustion. At 3 weeks after MR (5 weeks after PO), the exercise duration was shorter in the PO + VO group than in the sham or MR groups. At 9 weeks after MR (11 weeks after PO), the exercise durations became comparable between the VO only and the PO + VO groups, but both groups had shorter durations than the sham. However, interestingly, from 8 weeks after PO, the exercise duration significantly decreased in the PO group compared with the other groups (exercise duration at 14 weeks after PO, 735.3 ± 130.1 vs. 322 ± 56.2 vs. 447.8 ± 49.0 vs. 424.0 ± 80.3 seconds for sham vs. PO vs. VO vs. PO + VO, $p < 0.05$; **Figure 4B**).

Invasive hemodynamic measurement

At 14 weeks after PO, invasive hemodynamic assessment with a microtip P-V catheter system was performed. The PO + VO and VO groups had significantly dilated end-systolic volume (ESV), end-diastolic volume (EDV) and stroke volume (SV) compared with the sham and PO groups (**Table 1**). In addition, the end-systolic pressure-volume relationship (ESPVR) slope, known to be a load-independent index of LV contractile function, was not different among the sham, PO and PO + VO groups. However, the LV end-systolic (ESP) and end-diastolic pressure (EDP) and end-diastolic pressure-volume relationship (EDPVR) slope, an index of LV stiffness, were higher in the PO group than in the sham, VO and PO + VO groups (LV EDP; 10.5 ± 3.5 for sham, 14.5 ± 2.3 for PO, 10.2 ± 2.1 for PO + VO and 9.3 ± 2.3 for VO, $p < 0.05$, EDPVR slope; 0.010 ± 0.02 for sham, 0.161 ± 0.12 for PO, 0.034 ± 0.003 for PO + VO, 0.017 ± 0.01 for VO, $p < 0.05$; **Figure 5A**).

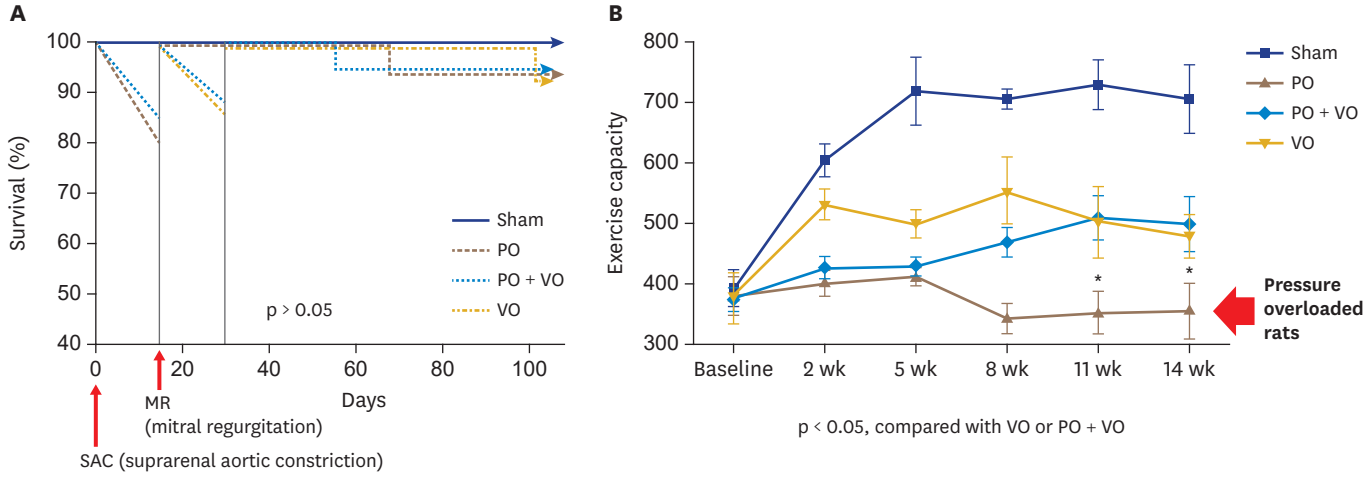

Figure 4. (A) Survival analysis. (B) Exercise capacity. MR: mitral regurgitation, PO: pressure overload, PO + VO: PO combined with VO, SAC: suprarenal aortic constriction, VO: volume overload, wk: week.

https://doi.org/10.4250/jcvi.2019.27.e4

Journal of Cardiovascular Imaging JCVI

Table 1. Invasive hemodynamic study

Variables	Sham	PO	PO + VO	VO
HR (beats/min)	321.5 ± 20.1	331.7 ± 24.7	325.4 ± 22.8	322.7 ± 24.7
EDV (mL)	430.9 ± 27.6	470.9 ± 27.1	979.7 ± 54.7	998.7 ± 54.7
ESV (mL)	127.2 ± 5.9	200 ± 4.9	310.2 ± 35.1	321.2 ± 37.1
EF (%)	70.2 ± 1.4	71.7 ± 3.5	65.2 ± 1.7	67.2 ± 3.7
SV (mL)	303.1 ± 21.0	280.4 ± 35.8	677.5 ± 48.5*	670.4 ± 35.8*
LV ESP (mmHg)	102.3 ± 7.5	145.4 ± 6.3	125.4 ± 4.0	105.4 ± 6.3
LV EDP (mmHg)	10.5 ± 3.5	14.5 ± 2.3	10.2 ± 2.1	9.3 ± 2.3
ESPVR (mmHg/μL)	0.032 ± 0.01	0.035 ± 0.02	0.030 ± 0.01	0.015 ± 0.01†
EDPVR (mmHg/μL)	0.010 ± 0.002	0.161 ± 0.001†	0.034 ± 0.003	0.017 ± 0.001

EDP: end-diastolic pressure, EDPVR: end-diastolic pressure-volume relationship, EDV: end-diastolic volume, EF: ejection fraction, ESP: end-systolic pressure, ESPVR: end-systolic pressure-volume relationship, ESV: end-systolic volume, HR: heart rate, PO: pressure overload, SV: stroke volume, VO: volume overload.
*$p < 0.05$ compared with sham and PO, †$p < 0.05$ compared with other groups.

Cardiac fibrosis and exercise capacity

Gross pathological examination showed that the heart was significantly enlarged with eccentric or concentric hypertrophy in the PO and the VO groups at week 14 of PO (**Figure 5B**). The extent of perivascular and interstitial fibrosis was significantly greater in the PO-only group than in the other group. Elevated EDPVR and cardiac fibrosis correlated with impaired exercise capacity (**Figure 5B**).

Microarray analysis

A total of 453 genes were differentially expressed by at least 1.5-fold in the PO + VO rats ($p < 0.05$), including 271 upregulated and 182 downregulated genes, compared with the VO or PO groups. The heat map in **Figure 6A** demonstrates a consistent pattern of change of these genes in each condition. For biological interpretation, we performed gene set enrichment analysis to explore the transcriptional changes at the level of molecular pathways or gene ontologies. **Figure 6B** is the network representation of gene sets that are enriched with genes upregulated and reciprocally downregulated between PO and VO. Transcriptional profiling of cardiac apical tissues revealed that gene sets related to the inflammatory response, DNA damage response, apoptosis, and cellular signaling pathways were significantly enriched by genes in the VO group, whereas cardiac fibrosis and cytoskeletal pathway and G-protein signaling genes were enriched in the PO group.

DISCUSSION

In the present study, we found that LVH created by suprarenal aortic constriction induced isolated diastolic dysfunction in rats (PO). In addition, we set up a new animal model with significant combined PO and VO. When we compared the effects of PO and the associated cardiac fibrosis on LV remodeling and exercise capacity in rats with significant VO, both the PO + VO and VO groups showed increased LV chamber size and reduced exercise tolerance to a similar degree as long-standing VO was continued. Unexpectedly, the PO group showed the worst exercise intolerance compared with the other groups, even PO + VO. Cardiac fibrosis was an important factor for exercise capacity and correlated with EDPVR. We found that many genes were regulated in PO, VO or both, and their regulation differed with cardiac remodeling. Cardiac fibrosis and the cytoskeletal pathway were important pathways in the PO group and appeared to be related to exercise capacity. Before reduced LV function, cardiac fibrosis might be associated with exercise capacity. To the best of our knowledge, this is the first study to perform serial echocardiographic follow-up and assess exercise

https://doi.org/10.4250/jcvi.2019.27.e4

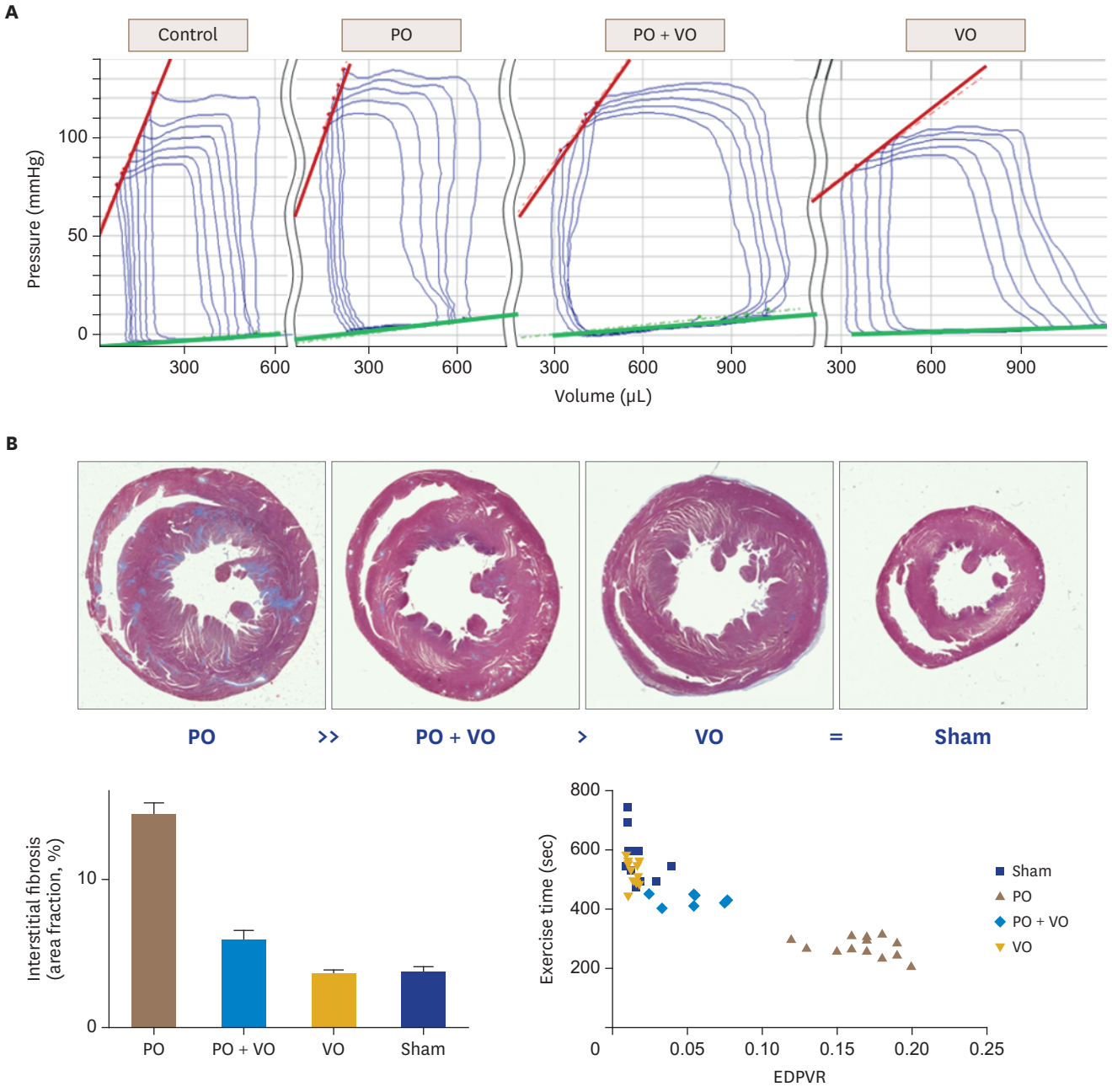

Figure 5. (A) A representative image of pressure and volume loop. (B) A representative image of histopathology. EDPVR: end-diastolic pressure-volume relationship, PO: pressure overload, PO + VO: PO combined with VO, VO: volume overload.

capacity in the chronic remodeling process caused by significant VO with or without PO and diastolic dysfunction.

Rats with a suprarenal aortic constriction as a model of PO associated with impaired diastolic function

To date, several animal models of cardiac hypertrophy with diastolic dysfunction have been reported. Doi et al.[8] reported that Dahl salt-sensitive rats fed a high-salt diet developed hypertension followed by LVH with diastolic dysfunction. However, most of them died of rapid progression of heart failure (HF). Because of their poor prognosis, they are used as

Journal of Cardiovascular Imaging JCVI

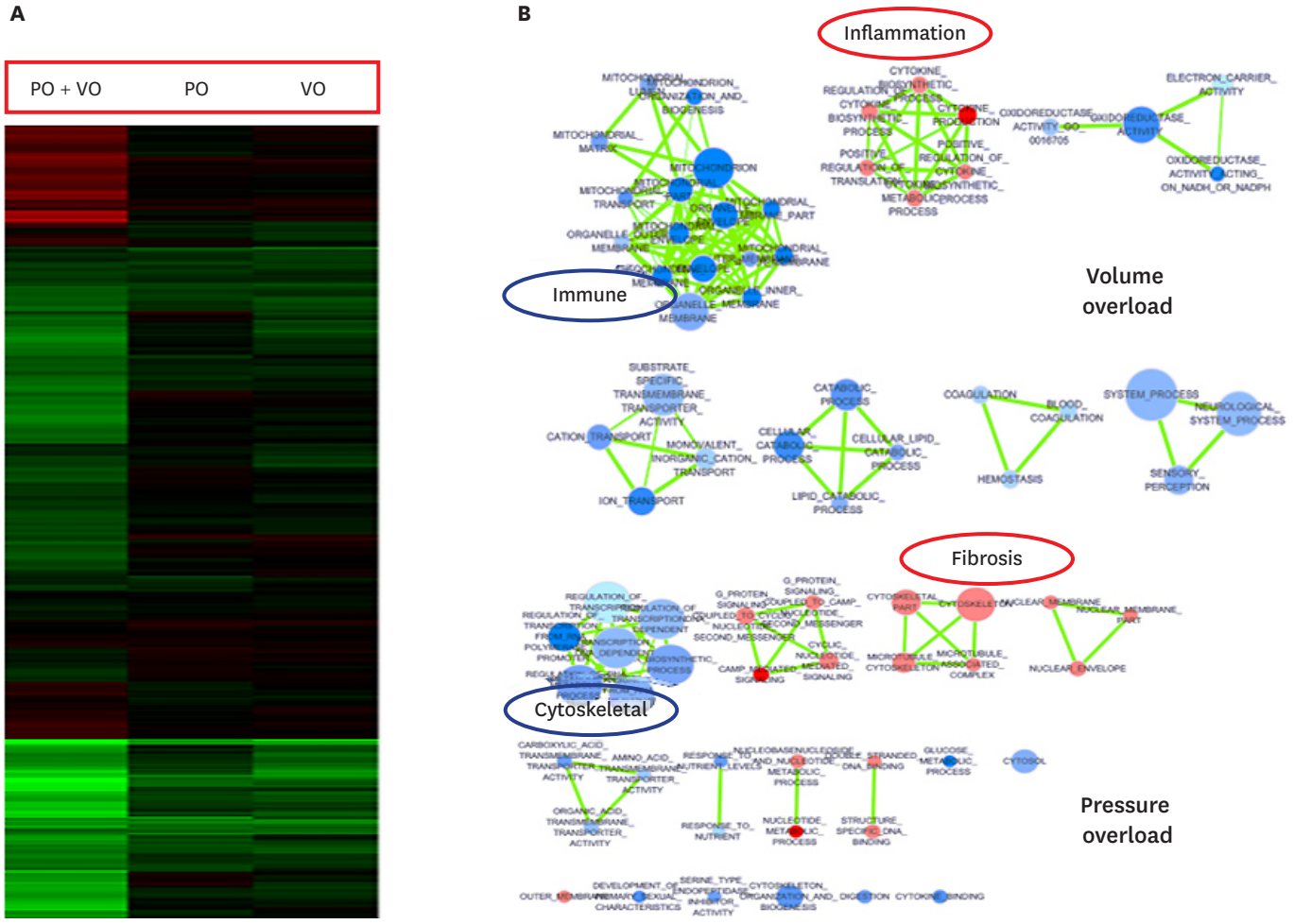

Figure 6. (A) The heat map of VO, PO and PO combined with VO. (B) Network of gene sets with significant enrichment scores. PO: pressure overload, PO + VO: PO combined with VO, VO: volume overload.

a model of isolated hypertensive diastolic HF, not isolated diastolic dysfunction. Another model of LVH and diastolic dysfunction was a rat model of suprarenal aortic constriction. It was reported that these rats did not show symptoms or signs of HF such as orthopnea, lung or liver congestion, and excessive weight gain until at least 16 weeks after suprarenal constriction.[9] When we followed the rats until 14 weeks after suprarenal aortic constriction, LVEF was not changed but LV wall thickness, as a marker of LVH, increased compared to the sham group. E/E', indicating the LV filling pressure, did not differ between the VO and PO groups. However, the E/E' ratio has been suggested to be an unreliable predictor of LV filling pressure in MR because of the load dependency of E velocity.[10] Additionally, the heart rates of the rats were so high that we could not sufficiently evaluate E/E'. This is why we did not follow up this parameter in the second round of experiments. We also confirmed the development of isolated diastolic dysfunction in this model through the invasive hemodynamic analysis. LV systolic parameters such as LVEF and the ESPVR slope did not differ between the PO group and the sham group. Among the diastolic parameters, only the LV EDP and the EDPVR slope increased in the PO group. In any case, we successfully created a rat PO model and isolated diastolic dysfunction, and this result encouraged us to further investigate in the setting of the combination of 2 models of PO and VO.

https://doi.org/10.4250/jcvi.2019.27.e4

Journal of Cardiovascular Imaging JCVI

An animal model of significant VO by mitral regurgitation

Next, we set up a rat model of MR with VO. Even though the incidence of MR is increasing,[11] the understanding of the mechanism of MR has been limited because of the absence of an adequate small animal model. Although large animal models (dogs or sheep) have been used for the experiments investigating the pathophysiology of MR, there have been too few subjects because of the high cost. We reported that a puncture of the mitral leaflet through the LV apex under the guidance of transesophageal echocardiography could lead to significant MR in rats.[5] This model has some advantages compared to large animal models. First, the costs are much lower. Second, they have a faster growth curve, so that LV remodeling and hemodynamic changes can be followed up in a shorter period. Third, the hard endpoints, such as the mortality, can be assessed.

In the present study, we could observe LV remodeling and relatively mild systolic dysfunction serially in the progression of MR. In addition, we could assess mortality of the MR rats. Approximately 10% of the rats died of MR immediately after the MR operation. However, no rats died during the rest of the study period. Interestingly, the hole in the mitral leaflet spontaneously regressed in rare cases, which were excluded from the analysis. Thus, serial echocardiographic confirmation of MR and direct visualization of the hole at the harvest time were important. However, contractile dysfunction has not been found in most experimental models of VO. Discrepancies between the normal contractile function found in experimental VO vs. the LV dysfunction found in clinical VO may relate to the experimental models employed to examine the problem. Additionally, VO in experimental models has usually been present for a shorter time than in humans, where VO may be tolerated for years to decades. Finally, ventricular dysfunction may be obscured if measured only at rest. It is possible that compensatory mechanisms such as adrenergic support could maintain ventricular function in the normal range at rest despite decreased cardiac reserve under stress.

Each model has strengths and weaknesses in terms of understanding the mechanisms responsible for HF, as well as developing effective new therapies for HF. Nonetheless, as noted earlier, our current models for understanding the mechanisms for HF are inadequate and do not provide an adequate scaffold for understanding newer device therapies that appear to work through neurohormonal-independent mechanisms.

The effect of PO on LV remodeling and exercise capacity in rats with significant VO and changes of gene sets

First, we monitored echocardiographic parameters including LV dimension, wall thickness, and LVEF until 12 weeks after MR formation (14 weeks after PO). LVESD and LVEDD were greater in the PO + VO and VO groups than in the PO or sham groups. LVEF was similarly reduced in the PO + VO group and the VO group at 12 weeks after MR formation. LVH continued in the PO + VO group during the study period. In the analysis of hemodynamic monitoring, the volumetric parameters such as LV ESV and LV EDV increased similarly in the PO + VO and the VO groups. Moreover, the diastolic parameters including the EDPVR slope were similar between the PO + VO group and the VO group. These results suggest that LV remodeling and associated diastolic dysfunction ultimately became similar under the different loading conditions. However, interestingly, the LV ESP and EDP and the EDPVR slope, an index of LV stiffness, were higher in the PO group than in the PO + VO group (EDPVR slope; 0.161 ± 0.12 for PO, 0.034 ± 0.003 for PO + VO, $p < 0.05$). Also, the extent of perivascular and interstitial fibrosis was significantly larger in the PO-group than in the PO + VO group. Elevated EDPVR and cardiac fibrosis correlated with impaired exercise capacity. We found the different gene sets among PO with VO, VO only group and PO only group.

https://doi.org/10.4250/jcvi.2019.27.e4

In the setting of PO, concentric LVH and fibrosis are produced and are related to diastolic dysfunction.[12][13] However, much less is known about the underlying mechanisms for remodeling due to VO compared with PO. A study reported that chronic VO might result in deposition of collagen and subendocardial fibrosis[14], and another study showed that VO of isolated MR decreased interstitial collagen as the first step of LV dilatation.[15-17] This uncertainty makes the interpretation of our results difficult. However, in the progression of LV remodeling, there is a pathway that is common to all kinds of loading conditions. Ryan et al.[16] and Stewart et al.[18] reported that eccentric LV remodeling in isolated MR was associated with increased matrix metalloproteinase (MMP) activity, using a gene array analysis. Moreover, even though concentric LVH was initially developed in PO, increased MMP activity gradually worsened LV remodeling, resulting in LV dilatation. MMPs are enzymes responsible for myocardial extracellular protein degradation in the failing heart, with their action restricted by tissue inhibitors of MMP (TIMPs). The disruption of MMP/TIMP balance has been observed to cause LV remodeling.[19][20] We induced MR before PO affected LV, and the increase in MMP activity affected LV remodeling. This may explain the similarities in LV dimensions, hemodynamic parameters, and consequent exercise intolerance between the PO + VO and VO groups. Because cardiac fibrosis may affect the PO only group more strongly than the PO + VO group, exercise capacity might be decreased severely in the PO only group. In other words, the time to activate genes was different between the PO and VO groups. The effect of PO and its associated diastolic dysfunction might be masked in the progression of LVH, which emphasizes the importance of timely correction of hypertension or PO before irreversible fibrosis occurs.

Study limitations

Some limitations of the present study should be acknowledged. First, MR was created by making a hole in the mitral leaflet, and this MR model may not represent VO in humans. This is an inherent limitation of animal models of HF. Second, we explained that cardiac fibrosis may be associated with exercise intolerance in the PO group. However, there might be many underlying mechanisms in LV remodeling such as the neurohumoral system, the formation of reactive oxygen species, and cytokines such as TGF-β. Third, our gene set data are the result of LV remodeling, not the cause. Thus, further investigation is needed to determine the molecular mechanism of LV remodeling in different loading conditions.

Conclusion

We investigated the effect of LVH and associated diastolic dysfunction on LV remodeling and exercise capacity. We found that many genes were regulated in PO, VO or both, and that there were differences in regulation by cardiac remodeling. Cardiac fibrosis and the cytoskeletal pathway were important pathways in the PO group and influenced exercise capacity. Before reduced LV function, cardiac fibrosis might be associated with exercise capacity.

ACKNOWLEDGMENTS

This research was funded by the Korea Society of Echocardiography Research Fund (2014).

REFERENCES

1. Konstam MA, Kramer DG, Patel AR, Maron MS, Udelson JE. Left ventricular remodeling in heart failure: current concepts in clinical significance and assessment. *JACC Cardiovasc Imaging* 2011;4:98-108.
PUBMED | CROSSREF

2. Yang DK, Choi BY, Lee YH, et al. Gene profiling during regression of pressure overload-induced cardiac hypertrophy. *Physiol Genomics* 2007;30:1-7.
PUBMED | CROSSREF
3. Miyazaki H, Oka N, Koga A, Ohmura H, Ueda T, Imaizumi T. Comparison of gene expression profiling in pressure and volume overload-induced myocardial hypertrophies in rats. *Hypertens Res* 2006;29:1029-45.
PUBMED | CROSSREF
4. Phrommintikul A, Tran L, Kompa A, et al. Effects of a Rho kinase inhibitor on pressure overload induced cardiac hypertrophy and associated diastolic dysfunction. *Am J Physiol Heart Circ Physiol* 2008;294:H1804-14.
PUBMED | CROSSREF
5. Kim KH, Kim YJ, Lee SP, et al. Survival, exercise capacity, and left ventricular remodeling in a rat model of chronic mitral regurgitation: serial echocardiography and pressure-volume analysis. *Korean Circ J* 2011;41:603-11.
PUBMED | CROSSREF
6. Kim KH, Kim YJ, Ohn JH, et al. Long-term effects of sildenafil in a rat model of chronic mitral regurgitation: benefits of ventricular remodeling and exercise capacity. *Circulation* 2012;125:1390-401.
PUBMED | CROSSREF
7. Pacher P, Nagayama T, Mukhopadhyay P, Bátkai S, Kass DA. Measurement of cardiac function using pressure-volume conductance catheter technique in mice and rats. *Nat Protoc* 2008;3:1422-34.
PUBMED | CROSSREF
8. Doi R, Masuyama T, Yamamoto K, et al. Development of different phenotypes of hypertensive heart failure: systolic versus diastolic failure in Dahl salt-sensitive rats. *J Hypertens* 2000;18:111-20.
PUBMED | CROSSREF
9. Kai H, Kuwahara F, Tokuda K, Imaizumi T. Diastolic dysfunction in hypertensive hearts: roles of perivascular inflammation and reactive myocardial fibrosis. *Hypertens Res* 2005;28:483-90.
PUBMED | CROSSREF
10. Olson JJ, Costa SP, Young CE, Palac RT. Early mitral filling/diastolic mitral annular velocity ratio is not a reliable predictor of left ventricular filling pressure in the setting of severe mitral regurgitation. *J Am Soc Echocardiogr* 2006;19:83-7.
PUBMED | CROSSREF
11. Nishimura RA, Otto CM, Bonow RO, et al. 2014 AHA/ACC guideline for the management of patients with valvular heart disease: a report of the American College of Cardiology/American Heart Association Task Force on Practice Guidelines. *J Am Coll Cardiol* 2014;63:e57-185.
PUBMED | CROSSREF
12. Moore-Morris T, Guimarães-Camboa N, Banerjee I, et al. Resident fibroblast lineages mediate pressure overload-induced cardiac fibrosis. *J Clin Invest* 2014;124:2921-34.
PUBMED | CROSSREF
13. Creemers EE, Pinto YM. Molecular mechanisms that control interstitial fibrosis in the pressure-overloaded heart. *Cardiovasc Res* 2011;89:265-72.
PUBMED | CROSSREF
14. Wang BW, Wu GJ, Cheng WP, Shyu KG. MicroRNA-208a increases myocardial fibrosis via endoglin in volume overloading heart. *PLoS One* 2014;9:e84188.
PUBMED | CROSSREF
15. Ulasova E, Gladden JD, Chen Y, et al. Loss of interstitial collagen causes structural and functional alterations of cardiomyocyte subsarcolemmal mitochondria in acute volume overload. *J Mol Cell Cardiol* 2011;50:147-56.
PUBMED | CROSSREF
16. Ryan TD, Rothstein EC, Aban I, et al. Left ventricular eccentric remodeling and matrix loss are mediated by bradykinin and precede cardiomyocyte elongation in rats with volume overload. *J Am Coll Cardiol* 2007;49:811-21.
PUBMED | CROSSREF
17. Chen YW, Pat B, Gladden JD, et al. Dynamic molecular and histopathological changes in the extracellular matrix and inflammation in the transition to heart failure in isolated volume overload. *Am J Physiol Heart Circ Physiol* 2011;300:H2251-60.
PUBMED | CROSSREF
18. Stewart JA Jr, Wei CC, Brower GL, et al. Cardiac mast cell- and chymase-mediated matrix metalloproteinase activity and left ventricular remodeling in mitral regurgitation in the dog. *J Mol Cell Cardiol* 2003;35:311-9.
PUBMED | CROSSREF

Journal of Cardiovascular Imaging JCVI

19. Franz M, Berndt A, Altendorf-Hofmann A, et al. Serum levels of large tenascin-C variants, matrix metalloproteinase-9, and tissue inhibitors of matrix metalloproteinases in concentric versus eccentric left ventricular hypertrophy. *Eur J Heart Fail* 2009;11:1057-62.
PUBMED | CROSSREF

20. Iwanaga Y, Aoyama T, Kihara Y, Onozawa Y, Yoneda T, Sasayama S. Excessive activation of matrix metalloproteinases coincides with left ventricular remodeling during transition from hypertrophy to heart failure in hypertensive rats. *J Am Coll Cardiol* 2002;39:1384-91.
PUBMED | CROSSREF

https://doi.org/10.4250/jcvi.2019.27.e4